Thermodynamic and Structural Investigations on the Different Forms of Syndiotactic Polystyrene Intercalates

Sudip Malik,[†,§] Cyrille Rochas,[‡] and Jean Michel Guenet*[,†]

Institut Charles Sadron, CNRS UPR 22, 6 rue Boussingault, BP 40016, F-67083 Strasbourg Cedex, France, and Laboratoire de Spectrométrie Physique, CNRS-UJF UMR5588, 38402 Saint Martin d'Hères Cedex, France

Received August 23, 2005; Revised Manuscript Received November 25, 2005

ABSTRACT: The occurrence of polymer−solvent intercalates of syndiotactic polystyrene (sPS) in biphenyl, benzophenone, and diphenylmethane has been observed from thermodynamic, structural, and morphological investigations. For each system the temperature−concentration phase diagram has been established by DSC and has allowed one to determine the number of sPS/solvent compounds. Experiments by X-ray diffraction and neutron diffraction bear out the outcomes of T−C phase diagrams of these systems. In addition, these diffraction experiments have shown that the highly solvated form, discovered in sPS/benzene systems [Daniel et al. *Polymer* **1996**, *37*, 1273], is more common than expected. We suggest to designate the usual chlathrate form as δ_c-form while the more solvated form could be named δ_i-form. Also, another form has been observed in these systems, which possesses a nematic-like order. As this form is also a sPS/solvent compound, we suggest to designate it as δ_N-form The morphology of each system significantly varies with the solvent.

Introduction

Syndiotactic polystyrene (sPS) which was first synthesized in the late 1980s[1,2] displays a very complex polymorphic behavior unlike isotactic polystyrene and particularly possesses the propensity of forming a wealth of polymer−solvent compounds. The polymorphic behavior of sPS has been extensively investigated by using differential scanning calorimetry (DSC),[3] Fourier transformed infrared (FTIR) spectroscopy,[4−6] wide-angle X-ray diffraction (WAXD),[7−9] etc. So far, four main crystalline forms have been identified: two crystalline forms, α and β, containing the all-trans conformation (planar zigzag) with identity period 0.51 nm and two forms, δ and γ, containing a 2_1 helical chain conformation with identity period of 0.77 nm.[9] Among the four crystalline forms of sPS, the δ-form consists of a polymer−solvent compound (also designated sometimes as crystallosolvates, intercalates, or chlathrates) and forms in a large variety of solvents such as benzene,[10] toluene,[11] chloroform, bromoform,[12] diethylbenzene,[13] naphthalene,[14] tetralin,[15] *trans*-decalin, etc., that are either liquid or solid at room temperature. Surprisingly enough, no significant change of the experimental lattice parameters have been observed hitherto despite the formation of sPS−solvent compounds with solvent molecules of highly differing shapes and sizes. Solvent molar volumes are ranging typically from 60 to 150 cm^3/mol, and molecules with shapes as different as 1,2-dichloroethane and *trans*-decalin produce virtually the same diffraction pattern.

The first observation of a different lattice, showing the existence of a second class of intercalates, was reported by Daniel et al.[10] for sPS/benzene. This structure could be described as a "swollen" form of the δ-form in the sense that the reflection at $q = 5.5$ nm^{-1} ($d = 1.14$ nm) is shifted to $q = 3.9$ nm^{-1} ($d = 1.61$ nm). Similar results were later reported by Rastogi et al.[16] and more recently by Petraccone et al.[17] These authors actually refer to the usual δ-form as chlathrates and the "swollen" form as intercalates. We shall suggest that the chlathrates could be designated as the δ_c-form while the "swollen" form designated as intercalates by Petraccone et al.[17] could be named the δ_i-form.

Here, we report on a similar class of sPS/solvent compounds that are prepared from solvents with molar volumes ranging from 150 to 168 cm^3/mol, for which the diffraction patterns significantly differs from that reported for the δ_c-form and resembles that of the δ_i-form. In addition to the δ_i-form, another form is observed which seems to possess a nematic-like order, and that we propose to designate as the δ_N-form.

In this paper we shall present the temperature−concentration phase diagram, the morphology, and the structure by time-resolved X-ray diffraction and by neutron diffraction of a series of samples prepared from closely related solvent molecules, namely sPS/biphenyl, sPS/benzophenone, and sPS/diphenylmethane. The chemical structures of three solvents are as follows: biphenyl (left), benzophenone (middle), and diphenylmethane (right).

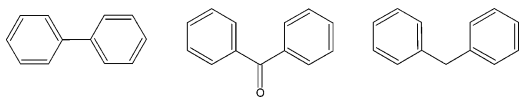

Experimental Section

Materials. The syndiotactic polystyrene (sPS) samples, hydrogenated (sPSH) and deuterated (sPSD), were synthesized following the method devised by Zambelli and co-workers.[1] The content of syndiotactic triads characterized by ^{1}H NMR was found to be over 99%. The molecular weight characterization of these samples was performed by GPC in dichlorobenzene at 140 °C and yielded the following data: $M_w = 1.0 \times 10^5$ with $M_w/M_n = 4.4$ for sPSH; $M_w = 4.3 \times 10^4$ with $M_w/M_n = 3.6$ for sPSD.

Hydrogenous and deuterated benzophenone, hydrogenous and deuterated biphenol, and hydrogenous diphenylmethane were purchased from Aldrich and were used without further purification.

† CNRS UPR 22.
‡ CNRS−UJF UMR5588.
§ Present address: Polymer Science Unit, Indian Association for the Cultivation of Science, Jadavpur, Kolkata 700032, India.
* Corresponding author: e-mail guenet@ics.u-strasbg.fr; Tel +33 (0) 388 41 40 87; Fax +33 (0) 388 41 40 99.

10.1021/ma051852s CCC: $33.50
Published on Web 01/07/2006

Techniques. *Differential Scanning Calorimetry.* The thermal behavior of the gel was investigated by means of a Perkin-Elmer DSC Diamond. The systems were systematically melted above 200 °C for 10 min and then cooled to −20 °C at 5 °C/min. Thermograms were recorded at heating rates of 5 and 2.5 °C/min. The phase diagrams were established on the basis of the thermograms obtained at the lowest heating rates. Possible kinetic effects, particularly on cooling the homogeneous solutions, were assessed by using different heating rates and cooling rates. The weight of the sample was checked after each experiment, and the instrument was calibrated with indium before each set of experiment.

For producing adequate DSC samples two procedures were employed. The first procedure was used for polymer fractions lower than $X_{pol} = 0.30$ g/g. Homogeneous solutions were prepared by heating at desired temperature in a hermetically closed test tube that contained a mixture of appropriate amounts of polymer and solvent. Pieces of the solid samples obtained after a subsequent cooling of these solutions at room temperature were then transferred to into "volatile sample" pan that were hermetically sealed. The systems were reheated to erase the thermal history and then cooled at controlled cooling rates in the DSC apparatus.

Mixtures of polymer fractions higher than $X_{pol} = 0.30$ g/g were prepared by allowing evaporation and/or sublimation of the solvent from the low-concentration sample (typically $X_{pol} = 0.30$ g/g) until the desired polymer fraction was reached as checked by weighing the sample. The samples were introduced into the DSC pan, hermetically sealed, and then subsequently heated to obtain a homogeneous system. The reliability of the second procedure was checked with samples prepared at $X_{pol} = 0.35$ g/g by both procedures.

Optical Microscopy. Optical investigations were carried out by means of Nomarsky phase contrast with a NIKON Optiphot-2 equipped with a CCD camera. Image processing and analysis were achieved by means of LUCIA, a software developed by Laboratory Imaging. The samples used for optical observation were prepared by remelting between glass slides those samples prepared beforehand in test tubes. To minimize solvent evaporation, the edge of the thin upper glass slide was glued with epoxy resin.

Scanning Electron Microscopy. A Hitachi S-2300 operating at a voltage ranging from 15 to 25 kV was used. A film of the sPS/naphthalene system was dried in a vacuum at room temperature, and it was coated with a gold layer of thickness 40 nm by sputtering technique in an argon atmosphere.

X-ray Diffraction. The X-ray experiments were performed on beamline BM2 at the European Synchrotron Radiation Facility (ESRF), Grenoble, France. The energy of the beam was 15.8 keV, which corresponds to a wavelength of $\lambda = 7.86 \times 10^{-2}$ nm. At the sample position the collimated beam was focused with a typical cross section of 0.1×0.3 mm^2. The scattered photons were collected onto a two-dimensional CCD detector developed by Princeton Instruments, presently Roper Scientific. Typical acquisition times are about 10−20 s, which allows time-resolved experiments to be carried out at 2 °C/min, a value close to the 2.5 °C/min heating rate used for DSC experiments.

The sample-to-detector distance was about 0.2 m, corresponding to a momentum transfer vector q range of $1 < q\ (\text{nm}^{-1}) < 17$, with $q = (4\pi/\lambda)\sin(\theta/2)$, where λ and θ are the wavelength and the scattering angle, respectively (further information is available on the Web site http://www.esrf.fr).

The scattering intensities obtained were corrected for the detector response, the dark current, the empty cell, the sample transmission, and the sample thickness. To obtain a one-dimensional X-ray pattern out of the two-dimensional digitalized pictures, the data were radially regrouped, and a behonate sample was used for determining the actual values of the momenta transfer q.

The sPS/solvent systems were prepared directly in glass tubes of 3 mm inner diameter and wall thickness 0.1 mm. After introducing a mixture of polymer and solvent these tubes were sealed from atmosphere in order to prevent from solvent loss. Homogeneous solution was obtained by heating that was eventually quenched to room temperature for producing the crystallized samples. To prevent possible artifacts from arising from evaporation, the tubes contained about 200−300 mg of sample, and the setup was so arranged that the X-ray beam crossed the sample right in its middle part.

Note that glass is virtually transparent to X-rays at the wavelength used.

Neutron Diffraction. Neutron diffraction can be an appropriate investigation tool for systems involving polymer−solvent compounds thanks to the deuterium-labeling possibility of either component. When dealing with a binary system, four labeling possibilities are accessible which provides one with four structure factors without significantly changing the molecular arrangement. The existence of polymer−solvent compounds can be demonstrated qualitatively by this technique,[18,19] as is illustrated by the general expression for the intensity diffracted by a binary system composed of one type of polymer and one type of solvent:

$$I(q) = A_p^2(q)\,S_p(q) + A_s^2(q)\,S_s(q) + 2A_p(q)\,A_s(q)\,S_{ps}(q) \quad (1)$$

where $A(q)$ and $S(q)$ with appropriate subscripts are the coherent scattering amplitude and the structure factor of the polymer (p) and of the solvent (s), and $S_{ps}(q)$ is a cross-term which is related to the coorganization of the polymer and the solvent.

Neutron diffraction experiments were carried out on D16, a two-circle diffractometer located at Institut Laue Langevin, Grenoble, France. This diffractometer is equipped with a position-sensitive ^{3}He multidetector with 128×128 wires. It operates at a wavelength $\lambda = 0.454$ nm obtained by diffraction of the neutron beam onto a pyrolytic graphite mosaic crystal (mosaicity = 0.7°) oriented under Bragg conditions (further details available at http://www.ill.fr). Momenta transfer $q = (4\pi/\lambda)\sin(\theta/2)$ rangedg from $q = 2$ to 17 nm^{-1}. Detector calibration and correction for cell efficiency were achieved with a spectrum given off by light water.

The compounds were prepared directly in amorphous quartz tubes of 3 mm inner diameter. After introducing a mixture of polymer and solvent, these tubes were sealed from the atmosphere. Homogeneous solution were obtained by heating and then were quenched to room temperature.

Results and Discussion

Preliminary Remarks. Before presenting and discussing the results for the three polymer/solvent couples, it is worth reminding that the reflections observed in diffraction experiments at $q = 5.5$, 7.4, 9.5, 9.83, and 11.8 nm^{-1} ($d = 1.13$, 0.85, 0.66, and 0.53 nm) are characteristic peaks for the δ_c form of sPS[4,7] (the solvated form made up with 2_1 helices) while the reflections at $q = 4.5$, 7.6, 8.6, 9.0, and 10.0 nm^{-1} ($d = 1.42$, 0.83, 0.73, 0.7, and 0.63 nm) stand for the signature of the β-form of sPS (the nonsolvated form with totally extended chains, namely the planar zigzag form). There exist variants of this form named β' and β''.

sPS/Biphenyl. The temperature−concentration phase diagram was established for a heating rate of 2.5 °C/min although rates of 5 °C/min were used for testing possible kinectic effects. Typical DSC traces are drawn in Figure 1. The thermal events around $T = 70$ °C are related to solvent melting while those at 90 °C and above 150 °C are related to the polymer. Worth noting is a small exotherm observed after the event at 90 °C at higher polymer concentration as was reported for the sPS/*trans*-decalin system.[15] The temperature−concentration phase diagram together with the Tamman diagram mapped out from the DSC traces are drawn in Figure 2. As is customary,[14,15,19−21] dashed lines represent plausible extensions determined on the basis of GIBBS phase rules. Three nonvariant events are observed: at $T = 70$ °C (endothermic), $T = 90$ °C (endothermic), $T = 100$ °C (exothermic), and above $T = 150$ °C (endothermic). Note that there is a splitting of the solvent melting endotherm, an effect related to the size of the solvent crystals.

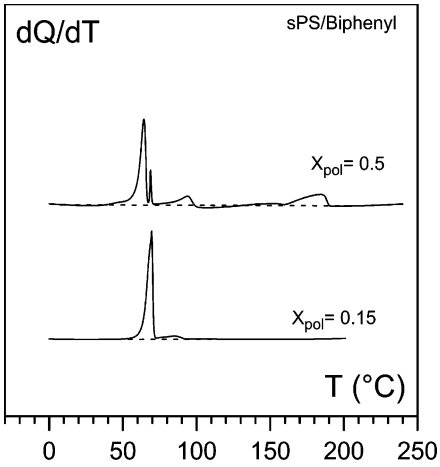

Figure 1. Typical DSC traces recorded for sPS/Biphenyl systems at 2.5 °C/min. Concentrations X_{pol} (w/w) as indicated.

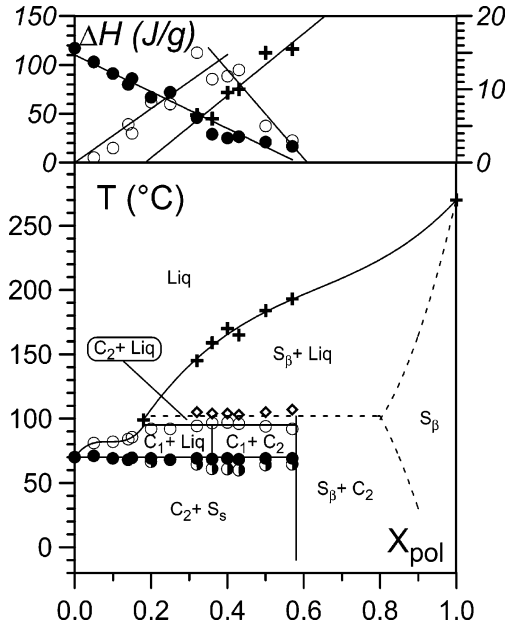

Figure 2. Temperature−concentration phase diagram (lower) and Tamman's diagram (upper) for sPS/biphenyl systems. There is a direct correspondence for the data points symbols in each diagram, except for the solvent melting enthalpy (○) which stands for the sum of the enthalpies of the two solvent melting events (◐ and ◑).

The shape and the variation of the enthalpies in the Tamman diagram suggest the existence of two sPS/solvent compounds and one solid phase. The maximum of the melting enthalpy ΔH_{90} of the event at 90 °C provides one with the "thermodynamic" stoichiometry of compound C_1, namely ~1 biphenyl/monomer (see Appendix for the definition of the "thermodynamic" stoichiometry vs structural stoichiometry). The concentration at which ΔH_{90} together with the melting enthalpy of the solvent becomes zero gives the "thermodynamic" stoichiometry of compound C_2, namely ~0.5 biphenyl/monomer.

Of further note is the transformation of compound C_1 into compound C_2 at the crystallization temperature of biphenyl. Again, this phenomenon has been observed with benzene and suggests that compound C_1 contains solvent molecules that are loosely bound as they eventually crystallize rather than remaining within the compound.

The terminal melting always consists of two endotherms as was already observed for other sPS/solvent systems. As the ratio of these endotherms is independent of the heating rate, it is thought that they correspond to different crystal sizes. Note that

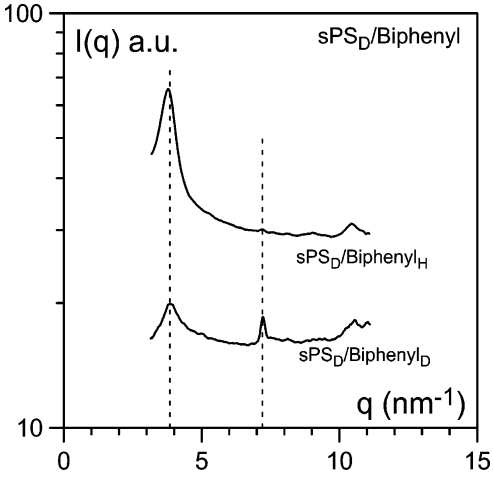

Figure 3. Neutron diffraction experiments performed at $T = 75$ °C: upper curve, $sPS_D/biphenyl_H$; lower curve, $sPS_D/biphenyl_D$; $X_{pol} = 0.40$ (w/w). To avoid the strong reflection from solvent molecules, we have plotted diffraction results for each system above the melting point of the corresponding solvent.

extrapolation to $X_{pol} = 1$ of the enthalpy associated with the melting of the solid-phase S_β gives $\Delta H = 35$ J/g, which suggests a crystallinity of about 50% if one takes $\Delta H_{sPS} \approx 75$ J/g, a value valid for all nonsolvated crystals of polyolefins.

On the basis of eq A2 (see Appendix), and a degree of crystallinity of about 50% for the compound, one has to consider a "stoichiometry" of the amorphous part for the intercalates of $S_{aC1} \approx 2.2$ solvent molecules/monomer if C_1 corresponds to the 1/2 structural stoichiometry, and $S_{aC2} \approx 0.75$, if C_2 corresponds to the 1/4 structural stoichiometry.

Finally, one has to consider another narrow domain, containing C_2 + liquid in order to fulfill Gibbs phase rules. The exothermic event at $T = 100$ °C might be related to the transformation of C_2 into S_β, more precisely to the transformation of the 2_1 helical form into the planar zigzag. As a matter of fact, this transformation is exothermic since the nonsolvated 2_1 helix is metastable.

The existence of sPS/biphenyl compounds is borne out by neutron diffraction experiments as shown in Figure 3. In these experiments the change from hydrogenous biphenyl to deuterated biphenyl entails a drastic change of the relative intensities between diffraction peaks. We further note that the first peak is observed at $q = 3.9$ nm$^{-1} \pm 0.1$, a value different from the usual δ-form but quite reminiscent of a value reported by Daniel et al. for benzene.[10] The time-resolved X-ray data obtained on these systems will provide one with additional information as to this new crystalline phase for sPS compounds. They are plotted in Figure 4 for $X_{pol} = 0.31$ (a), $X_{pol} = 0.43$ (b), and $X_{pol} = 0.50$ (c). As can be seen, the X-ray data are in excellent agreement with the DSC data, as one clearly sees the different transformation, in particular the β-form is observed at high temperature as expected.

The new form observed for C_1 has typical reflections at $q = 3.9 \pm 0.1$, 7.4 ± 0.1, 11, 14.1 ± 0.1, and 15.2 ± 0.1 nm^{-1} which totally differ from those reported for the usual δ-form but correspond to the solvated form reported by Daniel et al.[10] for sPS/benzene compounds. As mentioned in the Introduction section, we propose to name this form the δ_i-form, the subscript "i" indicating that more solvent molecules are intercalated between polymer stems on the basis of the crystal structure recently described by Petraccone et al.[17] Interestingly, in the case of the diffraction data for the highest concentration, one observes reflections which differ from the δ_i-form and the

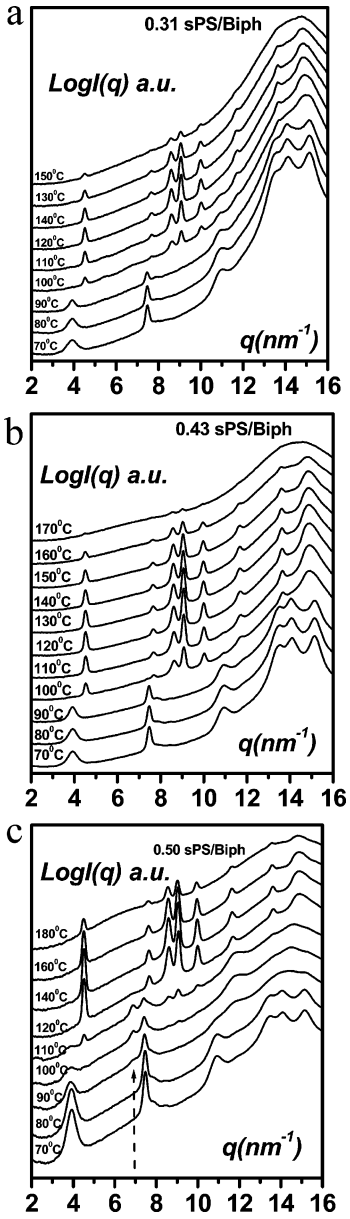

Figure 4. Time-resolved X-ray experiments as a function of temperature for three sPS/biphenyl systems: $X_{pol} = 0.31$ (a), $X_{pol} = 0.43$ (b), $X_{pol} = 0.50$ (c) concentrations in w/w. In (c) the arrow highlights the reflection at 6.8 nm^{-1}.

β-form. This structure, which corresponds to C_2 in the phase diagram, is characterized by two reflections: one, relatively sharp, at $q = 6.8 \pm 0.1$ nm^{-1} and a second, relatively broad, at $q = 11.8 \pm 0.1$ nm^{-1}. Note that the second broad reflection is already observable at lower temperature and should not be confused with the sharp reflection at $q = 11.6 \pm 0.1$ nm^{-1}, corresponding to the β-form as seen at higher temperature. We therefore suspect that C_2 is rather of the mesophase type (possibly a nematic-like structure). That the reflection at $q = 6.8 \pm 0.1$ nm^{-1} is not immediately seen just above the solvent melting point but is seen to appear at higher temperature in the $C_1 + C_2$ domain may arise from a gradual improvement of the order of the chains in this mesophase. This form could be named the δ_N-form to emphasize a probable nematic order.

SEM observations have revealed a fibrillar morphology after solvent removal at room temperature through sublimation (see Figure 5).

sPS/Benzophenone. As was emphasized in the Experimental Section, the DSC experiments were carried out by using a 2.5 °C/min heating rate on samples that had been cooled at the same rate. Typical DSC traces are shown in Figure 6.

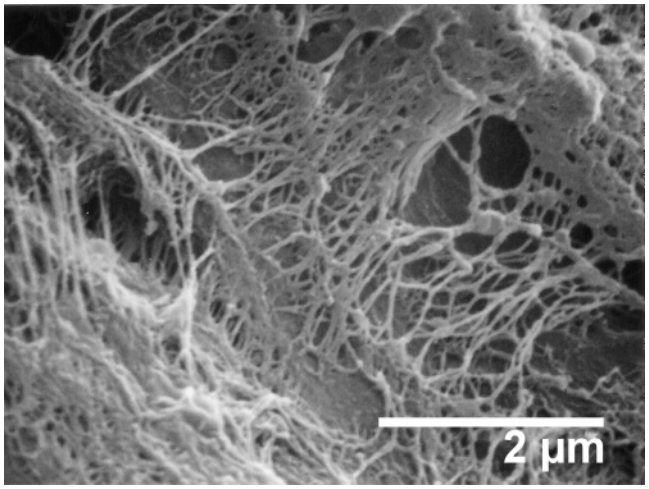

Figure 5. SEM micrographs for sPS/biphenyl systems for which the solvent has been sublimated at room temperature. $X_{pol} = 0.20$ (w/w). Scale as indicated.

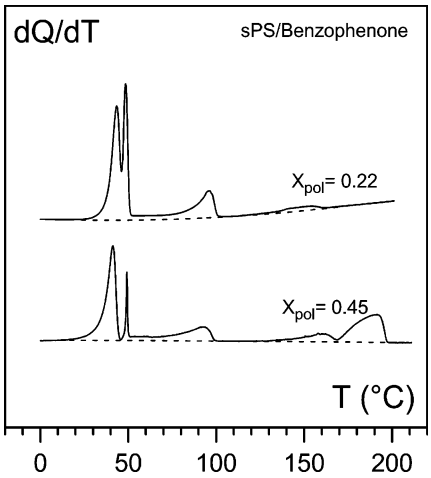

Figure 6. Typical DSC traces obtained for sPS/benzophenone systems at a heating rate of 2.5 °C/min. Concentrations X_{pol} (w/w) as indicated.

The temperature−concentration phase diagram together with Tamman's diagram mapped out from the DSC traces are drawn in Figure 7. As can be seen, three nonvariant events are observed at 40, 50, and 100 °C. The first two events are related to solvent crystallization, while the third corresponds to a solid transformation.

The Tamman diagram shows that the enthalpy ΔH_{100} related to the third nonvariant event at $T = 100$ °C departs from linearity in its ascending part, while a linear variation is observed in its descending part. The value of ΔH_{100} goes through a maximum at $X_{pol} = 0.43 \pm 0.03$ w/w. The total solvent melting enthalpy ΔH_s varies linearly and becomes zero for $X_{pol} = 0.6$ w/w. The enthalpy ΔH_T associated with the terminal melting increases linearly and extrapolates to zero for $X_{pol} = 0.21$. It amounts to $\Delta H_T = 40$ J/g after extrapolation to $X_{pol} = 1$ w/w, which, considering as above, that 100% crystallized sPS under the β-form would give $\Delta H_{sPS} = 75$ J/g, suggests a degree of crystallinity of sPS once under this form of about 53%. Note that, as above, the terminal melting always consists of two endotherms as was already observed for other sPS/solvent systems. The ratio of these endotherms is a constant as a function of the heating rate, so that they probably correspond to the melting of crystal with differing sizes. The existence of a maximum for ΔH_{100} is consistent with the existence of a

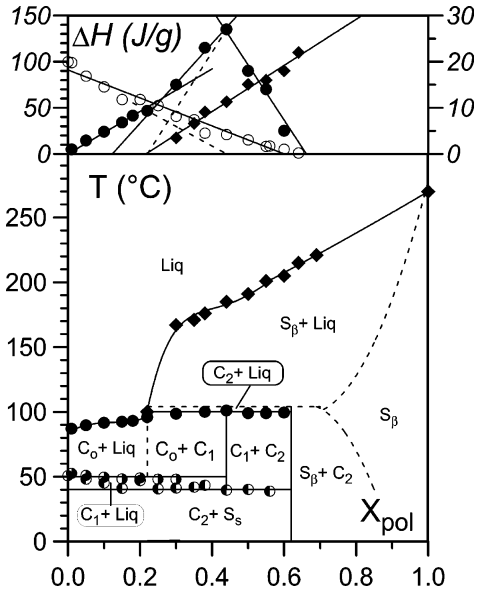

Figure 7. Temperature−concentration phase diagram (lower) and Tamman's diagram (upper) for sPS/benzophenone systems. There is a direct correspondence for the data points symbols in each diagram, except for the solvent melting enthalpy (○) which stands for the sum of the enthalpies of the two solvent melting events (◐ and ◑).

compound that we name C_1, with a "thermodynamic" stoichiometry 3 benzophenone/4 monomers (see Appendix). That both ΔH_{100} and ΔH_s become zero for the same concentration suggests the existence of another compound we name C_2, whose "thermodynamic" stoichiometry is 1 benzophenone/3 monomers. The fact that ΔH_{100} does not vary linearly in its ascending part suggests the existence of a third compound we name C_0. The use of different heating rates has shown this effect to be genuine. A similar situation has already been encountered by Saiani et al. in the case of syndiotactic PMMA.[22] Such a situation occurs when the melting peaks of each compound cannot be properly deconvoluted even by using very low heating rates. As a result, the enthalpy is the sum of two terms as highlighted with dashed lines in the Tamman diagram of Figure 7. Supposing the existence of a third compound, then its "thermodynamic" stoichiometry should correspond approximately to the zero of the terminal melting enthalpy, namely 2 benzophenone/monomer. For delimiting the domain of C_0 in the phase diagram a dashed line is used purposefully so as to stress that the existence of this compound only relies on the nonlinear variation of ΔH_{100} and must be considered as a plausible, yet not demonstrated, hypothesis. The two nonvariant events at the solvent melting temperature are consistent with the existence of this compound and suggest the following transformations:

$$C_2 + S \rightarrow C_1 + L \quad \text{and} \quad C_1 + L \rightarrow C_0 + L$$

where S is the solvent solid phase.

The occurrence of such transformations fulfills the rules derived by Gibbs for constructing phase diagrams. Similarly, there must be an additional domain above $T = 100$ °C where one has $C_2 + L$ in order to fulfill Gibbs phase rules. Admittedly, such a domain is likely to be hardly detectable by DSC experiments.

On the basis of eq A2 (see Appendix), and a degree of crystallinity of about 50% for the compound, one has to consider a "stoichiometry" of the amorphous part for the intercalates of $S_{aC1} \approx 1$ solvent molecules/monomer if C_1 corresponds to the 1/2 structural stoichiometry, and $S_{aC2} \approx 0.5$, if C_2 corresponds to the 1/4 structural stoichiometry. This means that in both cases

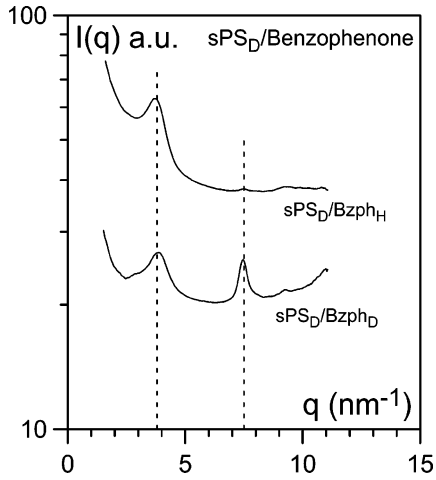

Figure 8. Neutron diffraction experiments performed at $T = 75$ °C: upper curve, sPS_D/benzophenone$_H$; lower curve, sPS_D/benzophenone$_D$; $X_{pol} = 0.41$ (w/w).

the amorphous domain contains the double of solvent molecules with respect to the organized part of the compound.

The existence of sPS/benzophenone compounds is given further support by neutron diffraction experiments, as shown in Figure 8. The change from hydrogenous benzophenone to deuterated benzophenone producs a drastic change of the intensities between diffraction peaks. Particularly, the peak at 7.5 ± 0.1 nm^{-1} virtually disappears when using deuterated benzophenone in lieu of hydrogenous benzophenone. As with biphenyl, the first peak observed at $q = 3.9 \pm 0.1$ nm^{-1} has a value different from the usual δ-form yet similar to that observed for sPS/benzene compounds.

The time-resolved X-ray data recorded on these systems are plotted in Figure 9 for $X_{pol} = 0.10$ (a), $X_{pol} = 0.30$ (b), and $X_{pol} = 0.59$ (c). Again, the X-ray data are in excellent agreement with the DSC data, as one clearly sees the different transformation, in particular the β-form is observed at high temperature as expected. Here, too, the diffraction pattern in the narrow T,C domain which is supposed to correspond to C_2 + liquid differs from that observed at lower temperature (the new form, see below) and at high temperature (the β-form).

The diffraction pattern for the domain where compounds C_0 and C_1 are supposed to coexist ($X_{pol} = 0.30$) has typical reflections at $q = 3.8 \pm 0.1$, 7.5 ± 0.1, 11 ± 0.1, 12.3 ± 0.1, 13.6 ± 0.1, 14.2 ± 0.1, and 15.1 ± 0.1 nm^{-1} that again totally differ from those reported for the usual δ_c-form but are close to those observed above for the δ_i-form.

Interestingly, at $X_{pol} = 0.59$ the diffraction pattern is reminiscent of what has been observed with sPS/biphenyl. We still observe the reflections corresponding to the δ_i-form ($q = 4 \pm 0.1$ nm^{-1}, 7.6 ± 0.1 nm^{-1}) and reflections corresponding to the δ_N-form observed above at 6.8 ± 0.1 and 11.8 ± 0.1 nm^{-1}. Note that reflections corresponding to the β-form are also present, although the phase diagram indicates that this form should not be there. It is probably a parasitic effect which may have two causes: (i) $X_{pol} = 0.59$ is very close to the stoichiometric composition, so that if the sample is slightly inhomogeneous more concentrated areas are likely to exist wherein the β-form will grow; (ii) because of the large size of the sample, some β-form may have formed due to inhomogeneity in cooling rate. One has to keep in mind that the diffracted intensity of the β-form is usually much stronger than the other forms.

A typical morphology of sPS/benzophenone systems is shown in Figure 10. The picture may suggest a fibrillar-like morphology although no clear-cut conclusions can be drawn, unlike what

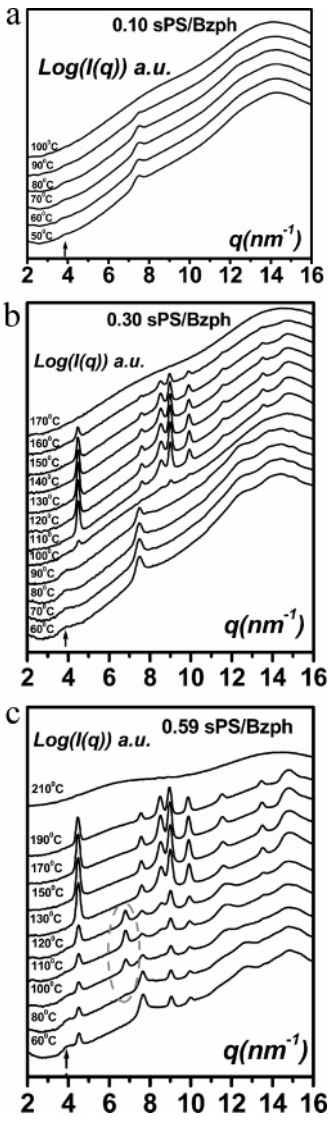

Figure 9. Time-resolved X-ray experiments as a function of temperature for three sPS/benzophenone systems: $X_{pol} = 0.10$ (a), $X_{pol} = 0.30$ (b), $X_{pol} = 0.59$ (c). Concentrations are in w/w. In (c) the dotted ellipse highlights the reflection at 6.8 nm^{-1}.

has been observed for sPS/biphenyl systems. Indeed, in some places features resembling a crumpled cloth are seen. We suspect that the way the solvent was removed could have affected the original fibrillar morphology. As a matter of fact, sPS/benzophenone samples for SEM investigations were prepared by cooling at room temperature only. Under these conditions, benzophenone is still in a liquid, metastable state, and its removal occurs through evaporation, not sublimation.

sPS/Diphenylmethane. Typical DSC traces are displayed in Figure 11. They are basically similar to those observed for sPS/biphenyl and sPS/benzophenone. The corresponding temperature−concentration phase diagram shown in Figure 12 is quite similar to that established for sPS/biphenyl as far as the overall shape is concerned. Here, too, the occurrence of two compounds is suggested. Compound C_1 has a "thermodynamic" stoichiometry of about 1 diphenyl methane/monomer against 1 diphenyl methane/3 monomers for compound C_2. Also, compound C_1 transforms into compound C_2 while solvent crystallizes. This again suggests that part of the solvent in compound C_1 is loosely bound.

Because of the nonavailability of deuterated diphenylmethane, no neutron diffraction experiments were performed.

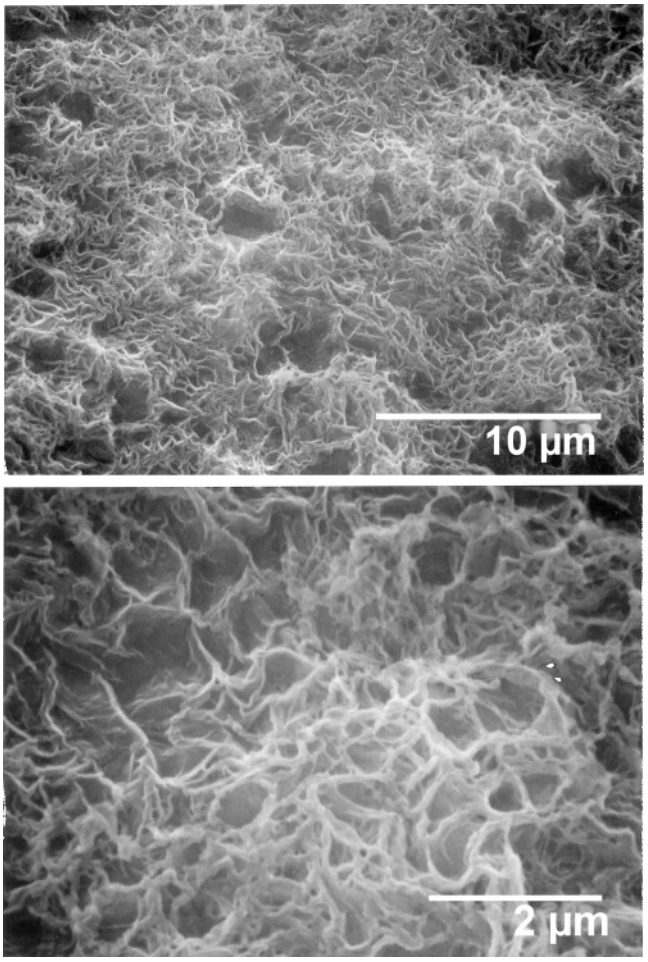

Figure 10. SEM micrographs for sPS/benzophenone systems for which the solvent has been evaporated at room temperature. $X_{pol} = 0.40$ (w/w). Scale bars as indicated.

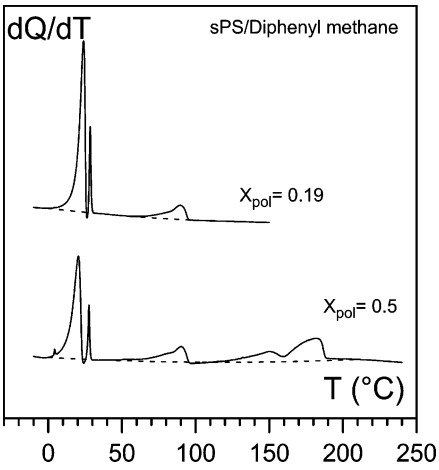

Figure 11. Typical DSC traces obtained for sPS/diphenylmethane systems at a heating rate of 2.5 °C/min. Concentrations X_{pol} (w/w) as indicated.

Time-resolved X-ray experiments are displayed in Figure 13 for $X_{pol} = 0.15$ (a) and $X_{pol} = 0.43$ (b). As with the above systems, reflections differing from the usual δ_c-form are observed and correspond rather to the δ_i-form. Typical reflections are seen at $q = 4 \pm 0.1$, 7.6 ± 0.1, 9.6 ± 0.1, 11.4 ± 0.1, 13.1 ± 0.1, 14.5 ± 0.1, 15.9 ± 0.1, and 17.1 ± 0.1 nm^{-1}. They slightly differ at the highest q values from the reflections observed for sPS/benzophenone and sPS/biphenyl, which indicates that there are variants of this δ_i-form.

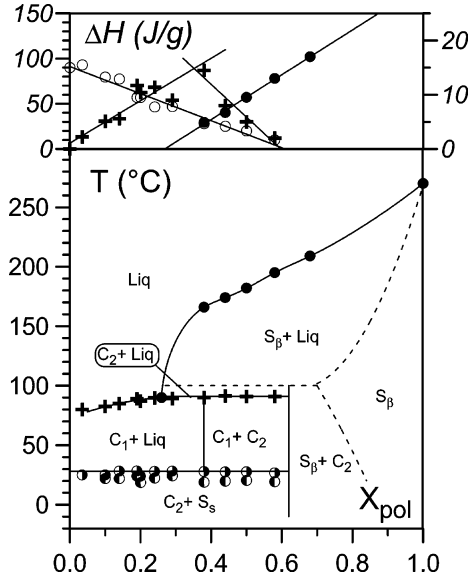

Figure 12. Temperature−concentration phase diagram (lower) and Tamman's diagram (upper) for sPS/diphenylmethane systems. There is a direct correspondence for the data points symbols in each diagram, except for the solvent melting enthalpy (○) which stands for the sum of the enthalpies of the two solvent melting events (◐ and ◐).

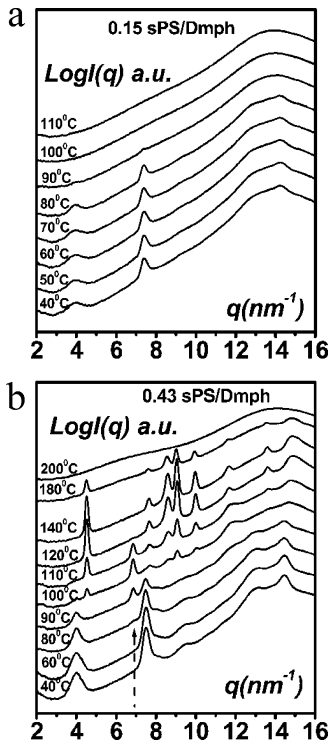

Figure 13. Time-resolved X-ray experiments as a function of temperature for three sPS/diphenylmethane systems: $X_{pol} = 0.15$ (a); $X_{pol} = 0.43$ (b). Concentrations are in w/w.

Here, too, an additional reflection appears at $q = 6.8 \pm 0.1$ nm^{-1} within a temperature range corresponding to the domain labeled C_2 + liquid. This again suggests the existence of a mesophase.

Interestingly enough, the morphology of sPS/diphenylmethane system is not fibrillar but spherulitic instead (see Figure 14). Normally, fibrillar morphology is thought to arise from the stabilization of the helical structure, and correspondingly of chain-folding impediment, by the solvation process, namely the occurrence of a polymer/solvent compound. In a previous paper, we suggested that the nature of the compound, which is

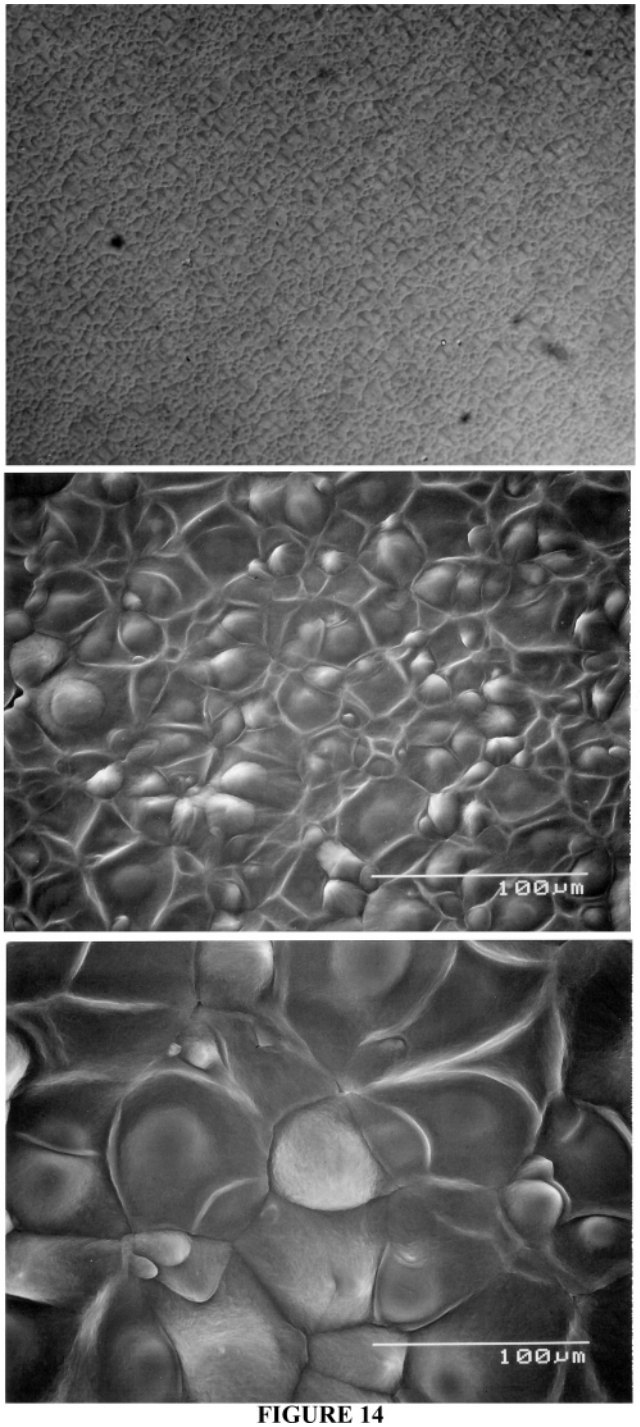

FIGURE 14

Figure 14. Optical micrograph (upper) and SEM micrographs (middle and lower) for sPS/diphenylmethane, $X_{pol} = 0.30$.

congruently melting or incongruently melting, could play a role in the degree of stabilization, the former being more efficient than the latter. The dissimilarity in morphology between sPS/biphenyl and sPS/diphenylmethane systems is therefore rather surprising as they exhibit very similar phase diagram. We, however, note that the crystallinity of the β-form as obtained from the extrapolation to $X_{pol} = 1$ for the terminal-melting enthalpy is of $X_c \approx 40\%$, which is slightly lower than that determined for the β-form of sPS/biphenyl systems. This may suggest that organization in sPS/diphenyl compounds is poorer than in sPS/biphenyl systems as the β-form results from the transformation of these solvated phases.

On the basis of eq A2 (see Appendix), and a degree of crystallinity of about 50% for the compound, one has to consider a "stoichiometry" of the amorphous part for the intercalates of $S_{aC1} \approx 1.4$ solvent molecules/monomer if C_1 corresponds to the 1/2 structural stoichiometry, and $S_{aC2} \approx 0.5$, if C_2 corresponds to the 1/4 structural stoichiometry.

Concluding Remarks

We have reported on a series of solvent wherein sPS form a type of compound first recognized for sPS/benzene systems,[10] which turns out to be more common than expected. We have also observed in the three systems a strong reflection at 6.8 ± 0.1 nm^{-1}, which corresponds to a domain of the phase diagram where the existence of another compound is expected. Most probably, this compound rather possesses a nematic-like structure so that we suggest to designate it as δ_N-form. The existence of such a form was already suggested by De Candia et al.[23]

Acknowledgment. IFCPAR-CEFIPRA is gratefully acknowledged for the financial support of this work (Grant No. 2808-2). The camera equipping the optical microscope together with the image processing software was financed through this grant. Sudip Malik is also indebted to IFCPAR-CEFIPRA (Grant No. 2808-2) for a postdoctoral fellowship. The authors are also greatly indebted for experimental assistance to Bruno DEME on D16 (ILL, Grenoble), to Christine Straupé on SEM, and to Catherine Saettel on DSC.

Appendix

From X-ray diffraction patterns[4] and FTIR on 1,2-dichlorodecane,[24] a structural stoichiometry 1 solvent molecules/4 monomers has been determined for the usual δ_c-form and 1 solvent molecules/2 monomers for the intercalates by Petraccone et al.[17] It should be stressed that, referring to the descriptions given in the experimental part, no proper control of the concentration was never achieved. We have recently noticed that concentration can dramatically be altered when transferring a small amount of material compound from the preparation tube into capillary tubes. This we observed while comparing neutron diffraction and X-ray diffraction experiments supposed to be carried out at the same concentration. The results were totally different as the δ_c-form was observed by neutron while the β-form was observed by X-ray. This was due to solvent evaporation as later X-ray experiments carried out on large quantities of samples directly prepared in sealed glass tubes, as were prepared the samples for neutron diffraction, were this time in agreement with neutron data (thanks to synchrotron radiation, experiments can be carried out in a wavelength range where glass is virtually transparent to X-rays).

The discrepancy between the stoichiometry determined from the phase diagram (that we will designate as "thermodynamic" stoichiometry) and that deduced from spectroscopic methods (X-rays, FTIR, etc.), namely the structural stoichiometry, may arise from the degree of solvation of the amorphous phase, particularly if the fraction of the latter is high. Clearly, this case may pertain to sPS.

From the temperature−concentration phase diagram, the stoichiometry of the compound S_c, namely the number of solvent molecules/monomer, is derived through[21]

$$S_c = \frac{1 - C_\gamma}{C_\gamma} \times \frac{m_p}{m_s} \qquad \text{(A1)}$$

where C_γ is the stoichiometric composition in w/w, and m_p and m_s are the molecular weights of the monomer and the solvent, respectively.

Now, if there exists a fraction of disorganized material, the stoichiometry of the compound S_c is written:

$$S_c = \frac{1 - C_\gamma[1 + (1 - X_c)S_a(m_s/m_p)]}{X_c C_\gamma} \frac{m_p}{m_s} \qquad \text{(A2)}$$

where S_a is the "stoichiometry" of the amorphous phase (also in terms of number of solvent molecules/monomer) and X_c is the degree of crystallinity. Three cases are worth contemplating: (i) If the fraction of the disorganized domains in the compound phase is low ($X_c \approx 1$), then relation A1 is retrieved, and what is determined by DSC corresponds virtually to the stoichiometry of the organized part of the compound. PEO complexes pertain to this category.[25] (ii) The number of solvent molecules/monomer is the same in the compound and in the disorganized domains; then one also retrieves relation A1, which means that the stoichiometry determined by DSC is the same as the stoichiometry of the complex. (iii) The number of solvent molecules/monomer is not the same in the compound and in the disorganized domains; then the stoichiometry derived from the $T-C$ phase diagram may not reflect the stoichiometry of the organized part.

References and Notes

(1) Grassi, A.; Pellechia, P.; Longo, P.; Zambelli, A. *Gazz. Chim. Ital.* **1987**, *117*, 249.
(2) Ishihara, N.; Seimiya, T.; Kuramoto, M.; Uoi, M. *Macromolecules* **1986**, *19*, 2465.
(3) Cimmino, S.; Pace, E. D.; Martuscelli, E.; Silvestre, C. *Polymer* **1991**, *32*, 1080.
(4) Chatani, Y.; Shimane, Y.; Inagaki, T.; Iijtsu, T.; Yukimori, T.; Shikuma, H. *Polymer* **1993**, *34*, 1620. Chatani, Y.; Inagaki, T.; Shimane, Y.; Shikuma, H. *Polymer* **1993**, *34*, 4841.
(5) Guerra, G.; Musto, P.; Karasz, F. E.; Mazknight, W. J. *Makromol. Chem.* **1990**, *191*, 2111.
(6) Gowd, E. B.; Nair, S. S.; Ramesh, C.; Tashiro, K. *Macromolecules* **2003**, *36*, 7388.
(7) Guerra, G.; Vitagliano, V. M.; De Rosa, C.; Petraccone, V.; Corradini, P. *Macromolecules* **1990**, *23*, 1539.
(8) Immirzi, A.; de Candia, F.; Ianelli, P.; Zambelli, A.; Vittoria, V. *Makromol. Chem. Rapid Commun.* **1988**, *9*, 761.
(9) Vittoria, V.; de Candia, F.; Ianelli, P.; Immirzi, A. *Makromol. Chem. Rapid Commun.* **1988**, *9*, 765.
(10) Daniel, C.; De Luca, M. D.; Brulet, A.; Menelle, A.; Guenet, J. M. *Polymer* **1996**, *37*, 1273.
(11) Daniel, C.; Brulet, A.; Menelle, A.; Guenet, J. M. *Polymer* **1997**, *38*, 4193.
(12) Rudder, J. D.; Berghmans, H.; Schryver, F. C. D.; Basco, M.; Paoletti, S. *Macromolecules* **2002**, *35*, 9529.
(13) Moyses, S.; Sonntag, P.; Spells, S. J.; Laveix, O. *Polymer* **1998**, *39*, 3665.
(14) Malik, S.; Rochas, C.; Guenet, J.-M. *Macromolecules* **2005**, *38*, 4888.
(15) Malik, S.; Rochas, C.; Schmutz,; M.; Guenet, J.-M. *Macromolecules* **2005**, *38*, 6024.
(16) Rastogi, S.; Goossens, J. G. P.; Lemstra, P. J. *Macromolecules* **1998**, *31*, 2983. van Hooy-Corstjens, C. S. J.; Magusin, P. C. M. M.; Rastogi, S.; Lemstra, P. J. *Macromolecules* **2002**, *35*, 6630.
(17) Petraccone, V.; Tarallo, O.; Venditto, V.; Guerra, G. *Macromolecules* **2005**, *38*, 6965.
(18) Klein, M.; Menelle, A.; Mathis, A.; Guenet, J.-M. *Macromolecules* **1990**, *23*, 4591.
(19) Point, J. J.; Damman, P.; Guenet, J.-M. *Polym. Commun.* **1991**, *32*, 477.
(20) Guenet, J.-M. *Thermochim. Acta* **1996**, *286*, 67.
(21) Klein, M.; Guenet, J.-M. *Macromolecules* **1989**, *22*, 3716.
(22) Saiani, A.; Spěváček, J.; Guenet, J. M. *Macromolecules* **1998**, *31*, 703.
(23) De Candia, F.; Guadagno, L.; Vittoria, V. *J. Macromol. Sci., Part B* **1995**, *34*, 95.
(24) Daniel, C.; Guerra, G.; Musto, P. *Macromolecules* **2002**, *35*, 2243.
(25) Wagner, J. F.; Dosière, M.; Guenet, J. M. *Macromol. Symp.* **2005**, *222*, 121. Tadokoro, H.; Yoshihara, T.; Chatani, Y.; Murahashi, S. *J. Polym. Sci., Part B* **1964**, *2*, 363.

MA051852S